

# The Effect of the Type and Composition of Demand on DSM Contribution to System Frequency Stability

# The Effect of the Type and Composition of Demand on DSM Contribution to System Frequency Stability

Mengxuan Wang, *Student Member, IEEE*, Jovica V. Milanovic, *Fellow, IEEE*
Department of Electrical and Electronic Engineering
The University of Manchester
Manchester, United Kingdom
mengxuan.wang@postgrad.manchester.ac.uk, milanovic@manchester.ac.uk

***Abstract*—In response to raising awareness about its potential contribution to system flexibility enhancement, Demand Side Management (DSM) is coming into research focus. However, due to the fact that DSM changes demand composition and hence load characteristics, it could have a significant influence on system dynamic behavior. This paper investigates the influence of DSM on system frequency stability by considering various types and compositions of load before and after DSM action. The results show that the same DSM action can result in different and even opposite impacts on system frequency stability depending on the underlying modelling of loads. The effect is illustrated on a modified version of the IEEE 68-bus test system with simulations performed in DigSILENT/PowerFactory environment.**

***Index Terms*—Demand side management, frequency stability, load composition, load modelling, probabilistic analysis.**

## I. INTRODUCTION

With the progressive decommissioning of fossil fuels and nuclear based synchronous power plants, and the ever-growing integration of renewable energy based generators, system inertia levels have been, or will be, reduced. Consequently, power system frequency stability may be affected. As one of the increasingly attractive potential solutions to maintain or enhance system frequency stability, Demand Side Management (DSM) came into prominence. It can adjust electricity consumption patterns, and subsequently compensate for the imbalance between power generation and load consumption such that the detrimental effects on system frequency stability performance could be mitigated. The potential of frequency support from aggregated domestic heat pumps and fridges has been estimated in [1], where a reduction of up to 50% of the spinning reserve capacity of conventional generators can be achieved in a simplified Great Britain system [1]. Likewise, the utilization of flexible loads to provide decentralized primary frequency reserves in a future Irish power system could lead to a 10% frequency nadir improvement following a contingency [2]. The deployment of DSM has been conducted in many European countries to provide ancillary services associated with frequency regulation [3].

However, due to the fact that DSM changes not only demand sizes, but also load compositions, system dynamic responses during frequency excursions could be affected significantly by the resulting load compositions. According to international survey results discussed in [4], many system operators are still using relatively simple and static load models for system dynamic simulations. The proliferation of power electronics connected generation and consequent reduction in system inertia will result in a change in system dynamic behavior, so there is a need to investigate more closely the effect of type, modelling and composition of demand on the potential impacts of DSM on system frequency stability.

This paper investigates the effect of load modelling and composition on the influence of DSM actions on power system frequency stability. Different types and compositions of load models are considered to establish to what extent is accurate load modelling, as integral part of any DSM programme, important when assessing the effects of DSM on frequency stability of power system. The system frequency responses are studied using probabilistic Monte Carlo based simulations, to account for system operational uncertainties resulting from renewable generation and demand variations. The results are illustrated using modified IEEE 68-bus test system with various renewable penetration and system loading levels.

## II. POWER SYSTEM FREQUENCY STABILITY

Power system frequency stability can be broadly defined as the ability of power systems to regain or maintain steady frequency when the system is subjected to a severe imbalance between generation and demand [5]. It is usually accessed and quantified by corresponding stability indices. Two frequency stability indices have been adopted in this study, namely frequency nadir and Rate of Change of Frequency (ROCOF).

Frequency nadir is the minimum frequency value during frequency excursions [5], while the definition of ROCOF associated with frequency nadir (as shown in (1)) is adopted in this study, where $f_{nadir}$, $f_{rated}$, $t_{nadir}$, and $t_{disturbance}$ are frequency nadir, system nominal frequency, time of frequency nadir and disturbance occurrences, respectively.

$$ROCOF\ (Hz/s) = \frac{|f_{nadir} - f_{rated}|}{t_{nadir} - t_{disturbance}} \quad (1)$$

## III. SYSTEM UNDER STUDY

### A. Test System Model

A modified version of IEEE 68-bus NETS-NYPS (New England Test System – New York Power System) network has been adopted in this study. The test network, as shown

in Fig. 1, has been divided into five areas interconnected by eight tie-lines. In total 12 (loads at buses 33, 36, 40, 41, 42, 50, 52, 56, 59, 60, 61 and 64) out of 35 loads are defined as large industrial customers, while all remaining loads are allocated to the distribution network (DN). Also, in order to appropriately distinguish the different power consumption patterns of large industrial customers and DNs, and the different generation characteristics of wind turbines and photovoltaics (PV), normalized daily loading curves for all load categories [6] and normalized renewable output curves [7] have been considered and modelled in the test network. Further information related to the test network can be found in [8].

### B. Modelling of System Operational Uncertainties

As the consequence of the intermittent and stochastic nature of renewable generations, as well as temporally and spatially varying load consumptions, modern power systems are operating with a huge amount of uncertainties. In this study, a Weibull distribution with α = 2.2 and β = 11.1 [9] and a Beta distribution with a = 13.7 and b = 1.3 [10] are used to represent the wind speed and PV output, respectively. Furthermore, system load demand follows a normal distribution, where the mean value is determined based on the normalized loading curves mentioned above and the standard deviation is assumed to be 3.33% [11]. The above system operational uncertainties are sampled independently, from corresponding probability distributions, in Monte Carlo simulations.

### C. Modelling of Load

In order to study the influence of load modelling, three different load models are considered, namely classical static load model, polynomial ZIP load model and a composite load model. A composite load model consists of parallel connection of static ZIP load (as shown in (2) and (3)) and a dynamic induction motor (IM). Where ZIP load is modelled as an aggregation of constant impedance (Z), constant current (I) and constant power (P) loads, and IM are considered as aggregation of individual IMs each rated at 5 kW [12].

$$P = P_n(a(V/V_O)^0 + b(V/V_O)^1 + c(V/V_O)^2) \quad (2)$$

$$Q = Q_n(a(V/V_O)^0 + b(V/V_O)^1 + c(V/V_O)^2) \quad (3)$$

In (2) and (3), rated active power, rated reactive power and rated voltage of loads are represented by $P_n$, $Q_n$ and $V_o$, respectively. Load composition can be adjusted by changing the values of parameters $a$, $b$ and $c$, depicting coefficients for P, I and Z loads, respectively, and the number of aggregated IM [12].

Furthermore, the daily variation of load composition for large industrial customers is adopted from [13], while the composition of DN is determined based on the CREST tool reported in [14]. Only the IM component of the demand and a part of the Z load are considered controllable in this study. Frequency dependency of the load is modelled as (4) and (5) for purely Z, I or P loads, and (6) to (8) for ZIP load.

$$P = P_n(V/V_O)^{k^p}(f/f_o)^{k^{pf}} \quad (4)$$

$$Q = Q_n(V/V_O)^{k^q}(f/f_o)^{k^{qf}} \quad (5)$$

$$P = P_n\left(a(V/V_O)^0 + b(V/V_O)^1 + c(V/V_O)^2\right)\left(1 + k^{pf}\Delta f\right) \quad (6)$$

$$Q = Q_n\left(a(V/V_O)^0 + b(V/V_O)^1 + c(V/V_O)^2\right)\left(1 + k^{qf}\Delta f\right) \quad (7)$$

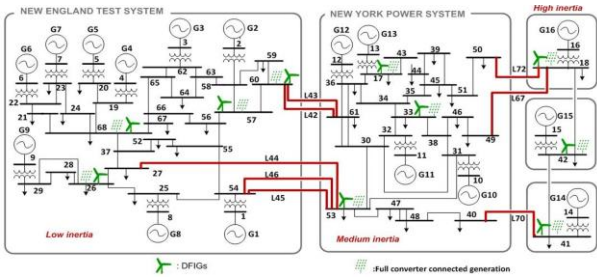


Figure 1. Test Network (Modified IEEE 68-Bus NETS-NYPS System)

$$\Delta f = (f - f_o)/f_o \quad (8)$$

Where $P_n$, $Q_n$ and $V_o$ have been defined in (2) and (3), $f_o$ is the system nominal frequency (50 Hz or 60 Hz), $k^p$ and $k^q$ are exponential coefficients used to determine the load type, while $k^{pf}$ and $k^{qf}$ describe the change in load demand in response to variations in frequency [4]. For (4) and (5), $k^{pf}$ =2.6, $k^{qf}$ =1.6 and $k^{pf}$ =1, $k^{qf}$ =-1.5 are adopted for large industrial customers and DNs, respectively [4]. In the case of (6) and (7), $k^{pf}$ and $k^{qf}$ are assumed to be 0.3398 and 3.355, respectively [4].

## IV. Research Methodology

### A. Implementation of DSM Actions

The DSM implemented in this study is essentially load shifting, i.e., system load demand is curtailed during peak hours (when demand is higher than 1.1 × average value of daily load demand), and increased during off-peak hours (when demand is lower than 0.85 × average value of daily load demand) [12]. The total system loading curves without and with DSM applications, as well as upper threshold and lower threshold defined as 1.1 × and 0.85 × average value of daily load demand, respectively, are illustrated in Fig. 2.

When all loads in the system are modelled as purely static loads, the adjustment of load demand is conducted by varying the values of $P_n$ and $Q_n$ in (2) and (3). The total DSM capacity at each hour is divided into 35 different values (there are 35 loads in the test network) based on (9) and these values are allocated to corresponding loads such that each load has a different DSM capacity at a different hour.

$$\text{DSM capacity of load}_i = \frac{Demand\ of\ Load\ i}{Total\ System\ \ Load\ Demand} \times \text{DSM capacity} \quad (9)$$

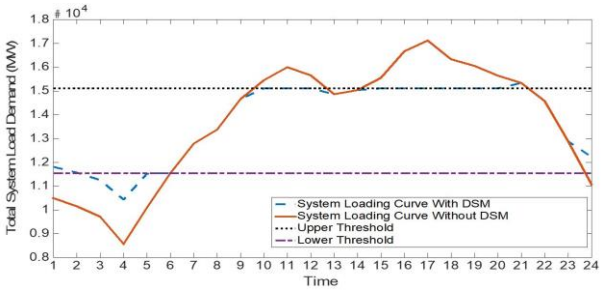


Figure 2. System Loading Curves Before/After DSM Actions [6, 12]

In the case of a composite load model (ZIP load in parallel with IM load), the same amount of load at a particular bus is connected or disconnected at different hours as before. However, due to the existence of static and dynamic loads, the controllable load is further segmented

into controllable Z loads and IM at each bus. $P_n$, $Q_n$ and all coefficients ($a$, $b$ and $c$) in (2) and (3), as well as the aggregation number of individual IM are re-calculated in order to appropriately account for the variation of load composition from the bus.

### B. Monte Carlo Based Probabilistic Simulation

For the purpose of performing probabilistic simulations covering the system operational uncertainties, a Monte Carlo based probabilistic analysis method was implemented in this study. First, scaling factors associated with system uncertainties following corresponding probability distributions are generated in Matlab using independent Monte Carlo sampling. The optimal power flow (OPF) is then performed in the Matpower [15] for each sampled set of data to determine the dispatch of conventional generators. Following this, the OPF results are imported from Matlab to DigSILENT PowerFactory and corresponding dynamic simulations are carried out. Finally, frequency nadir and ROCOF are calculated in Matlab from obtained frequency responses for each set of 100 Monte Carlo samples [16]. Since this was an exploratory and illustrative study only, 100 Monte Carlo samples were deemed to be sufficient.

The impact of DSM on power system frequency stability is quantified by changes of the frequency nadir and ROCOF, where percentage changes are evaluated by (10). Moreover, as a result of Monte Carlo simulation, a set of statistical values including mean values, median values and the most probable values, are utilized to derive general effects of DSM from vast amounts of simulation results.

$$Change\ (\%) = \frac{Indices\ Before\ DSM - Indices\ After\ DSM}{Indices\ Before\ DSM} \times 100\% \quad (10)$$

### C. Study Cases

In total three study cases have been developed with different renewable penetration and loading levels, all study cases are listed in Table I.

TABLE I. STUDY CASES

| Case No. | Renewable Penetration Level | System Loading Level | System Inertia Constant |
|---|---|---|---|
| 1 | 30% | 100% | 6.09 s |
| 2 | 60% | 100% | 4.07 s |
| 3 | 60% | 60% | 2.64 s |

All cases are developed in order to study the frequency response under different system inertia levels with frequency dependency. Connection of renewable generators and system de-loading could lead to a reduction in system inertia levels, which is modelled as a reduction of the apparent powers of synchronous generators in the test network. System de-loading is achieved by decreasing all loads evenly and simultaneously. According to (9), system de-loading could also reduce DSM capacity of the load, and such limit its ability to provide stability support by adjusting its demand.

In addition, three different load types are adopted in each study case, namely constant impedance load, constant power load and composite load model. The coefficients in (2) and (3) are modelled as $c = 1, a = b = 0$ and $a = 1, b = c = 0$ for constant impedance and constant power load, respectively. In the case of the composite load model, coefficients $a, b$ and $c$ are varying at different bus and hours to reflect different load compositions. Last but not least, by assuming that only IM and a part of Z load are controllable, it is only in the case of the composite load model that load composition can change with the application of DSM.

## V. SIMULATION RESULTS AND ANALYSIS

For the purpose of investigating the impact of DSM on system frequency stability, a disturbance is introduced into the system. The disconnection of G11 (see Fig. 1), which can lead to about a 6% drop of generated power, depending on different renewable penetration and loading levels, is chosen as the system disturbance. The disturbance is always introduced at 1s while the whole simulation is performed for 20s. The frequency responses of L42, one of the tie lines in the system, was selected to illustrate the overall frequency stability performance of the system as the lowest frequency nadir was observed across this line.

### A. Effects of Load Models

Three different load models, namely constant impedance, constant power and composite, have been adopted in this study to investigate the impact of load models on the influence of DSM on power system frequency stability. The mean values of the percentage changes of frequency nadir with different load models in Cases 1, 2 and 3 are illustrated in Fig. 3, Fig. 4 and Fig. 5, respectively. Hours 10 to 12 and Hour 15 have been omitted from all figures for their practically insignificant variations on stability indices caused by DSM actions.

It can be seen from Fig. 3 to Fig. 5 that different load models can lead to quite different, or even opposite impacts of DSM on frequency nadir. Opposite impacts of DSM due to the application of different load models can be observed at Hour 16 of Case 1 (Fig. 3) and Hours 20 and 21 of Case 3 (Fig. 5). Moreover, the differences in the impact of DSM caused by load models are more significant during load reconnection hours and in a system with higher inertia levels (Case 1 and Case 2).

From Fig. 3 and Fig. 4, it can be seen that an increase of renewable generation can enlarge the impacts of DSM on system frequency stability, i.e., DSM is more effective in renewable generation rich network. On the other hand, from Fig. 4 and Fig. 5, it can be seen that system de-loading can reduce the influence of DSM, which is the consequence of reduced real DSM capacity with system de-loading.

Additionally, the composite load model is the most influential in terms of the influence on frequency nadir because it results in the highest sensitivity of frequency nadir to DSM actions in most cases (Cases 2 and 3).

In terms of ROCOF, the mean value of absolute changes in ROCOF with different load models and frequency dependency in Cases 1, 2 and 3 are shown in Fig. 6, Fig. 7 and Fig. 8, respectively. Similar to frequency nadir, opposite impacts of DSM as results of different load models can be observed at 2 out of 12, 6 out of 12, and 4 out of 12 DSM application hours in Case 1 (Fig. 6), Case 2 (Fig. 7) and Case 3 (Fig. 8), respectively. Among all DSM application hours, these opposite impacts of DSM appeared more commonly in load curtailment hours, especially hours with large load curtailment capacities (Hours 17 to 21), which emphasizes the importance of adopting accurate and realistic load models in dynamic studies investigating the impacts of load curtailment on system frequency stability performance.

Focusing on Fig. 6 to Fig. 8, composite load model can be considered again as the most critical load model regarding ROCOF because it is more sensitive to DSM actions in almost all conditions. In all cases considered in this sub-section, the detrimental effects on frequency stability as a result of load reconnection are usually much severer than the enhancement of frequency stability contributed by load curtailments in the case of composite load model. ROCOF has increased by up to 0.096 Hz/s, 0.084 Hz/s and 0.076 Hz/s in Cases 1, 2 and 3, respectively, as the consequence of load reconnection. Last but not least, it can be noticed from Fig. 6 to Fig. 8 that larger DSM capacities usually lead to a more significant effect of DSM on system frequency stability performance.

The large differences in the results observed in both, changes in frequency nadir and ROCOF, following the DSM action with different load models could lead to inappropriate setting of system protection and control devices hence the need for an accurate representation of load in DSM studies.

### *B. Effects of Load Compositions*

Only a composite load model is used in this section as only that can enable variations of load composition after the application of DSM. The mean, median and the most probable values of absolute changes to ROCOF in Cases 1 is presented as Fig. 9. With respect to the different statistical values used to describe the effects of load composition on frequency performance indicators following the DSM, it can be concluded from Fig. 9 that in most cases they provide the same information and can be used interchangeably. Therefore, only the most probable values of absolute changes to ROCOF in Cases 2 and 3 are presented as Fig. 10 and Fig. 11, respectively.

As can be seen from Fig. 9 to Fig. 11, even though DSM applications in this case adjust load compositions at each load reconnection hours to a unique combination of static and dynamic loads, load reconnection always deteriorates system ROCOF and the effect is usually more pronounced in the case of higher DSM capacities (amounts of load reconnection).

However, during load curtailment hours, the impact of DSM on ROCOF could vary due to the different load compositions. The ROCOF is mostly improved during load curtailment hours (see Fig. 9 to Fig. 11) and the extent of the improvement depends on the penetration levels of renewable generation. A larger penetration of renewable generation resulted in a greater improvement of ROCOF during the load curtailment hours. To sum up, load composition plays a more significant role during load curtailment hours and it affects both magnitude and direction of the change in ROCOF.

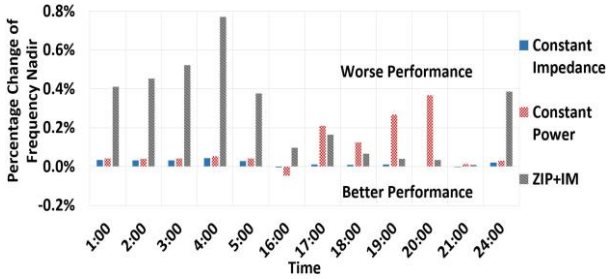


Figure 3. Mean Value of Percentage Change of Frequency Nadir with Different Load Models in Case 1 (30% Renewable and 100% Loading)

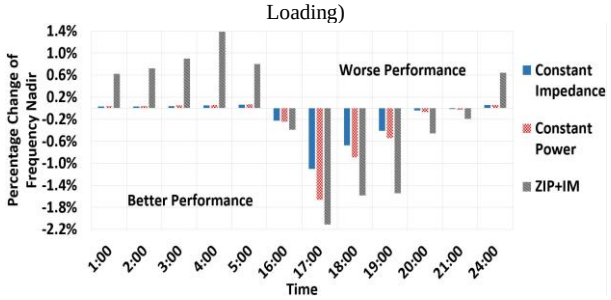


Figure 4. Mean Value of Percentage Change of Frequency Nadir with Different Load Models in Case 2 (60% Renewable and 100% Loading)

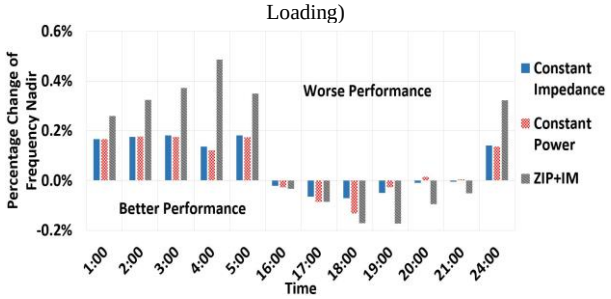


Figure 5. Mean Value of Percentage Change of Frequency Nadir with Different Load Models in Case 3 (60% Renewable and 60% Loading)

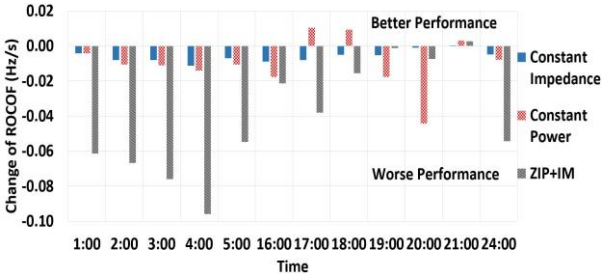


Figure 6. Mean Value of Absolute Change of ROCOF with Different Load Models in Case 1 (30% Renewable and 100% Loading)

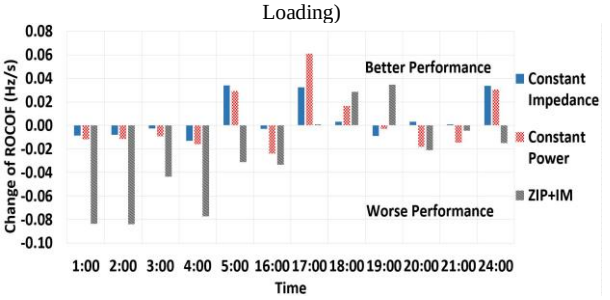


Figure 7. Mean Value of Absolute Change of ROCOF with Different Load Models in Case 2 (60% Renewable and 100% Loading)

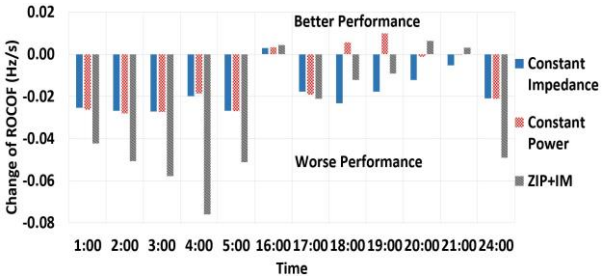


Figure 8. Mean Value of Absolute Change of ROCOF with Different Load Models in Case 3 (60% Renewable and 60% Loading)

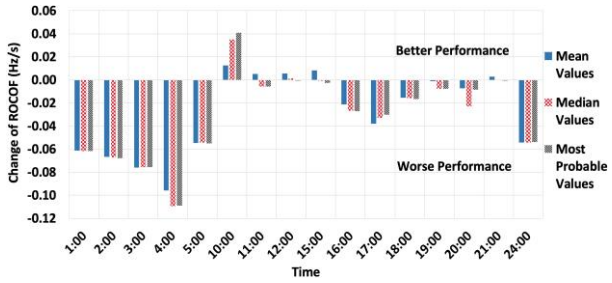


Figure 9. Mean Value, Median Values and Most Probable Values of Absolute Change of ROCOF with Composite Load Models in Case 1 (30% Renewable and 100% Loading)

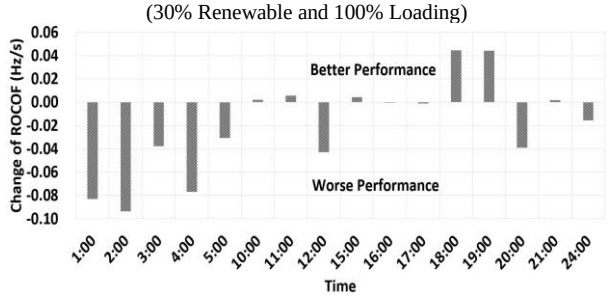


Figure 10. Most Probable Values of Absolute Change of ROCOF with Composite Load Models in Case 2 (60% Renewable and 100% Loading)

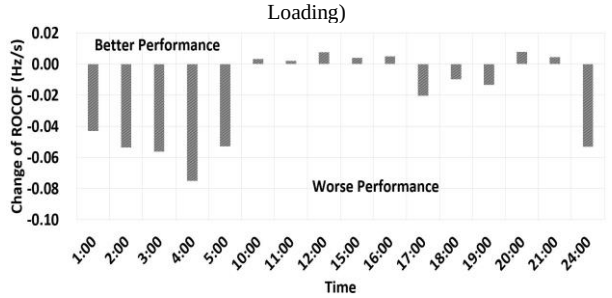


Figure 11. Most Probable Values of Absolute Change of ROCOF with Composite Load Models in Case 3 (60% Renewable and 60% Loading)

## VI. CONCLUSIONS

This paper illustrated that the same DSM action can lead to different and even opposite impacts on system frequency nadir and ROCOF depending on the adopted load model and composition. The use of composite load model resulted in the biggest changes in frequency nadir and ROCOF. The load composition is found to be much more relevant to model during the load curtailment hours as bigger effect of load composition was observed during these times. This preliminary study indicated that the inappropriate modelling of load both in terms of load models used and the composition of demand, could result in an inaccurate assessment of the influence of DSM on system frequency stability. This could affect the efficient deployment of DSM to support the operation of power system with large penetration of RES. The extent of the observed effect is system dependent. Further, more accurate modelling of system dynamics during connection and disconnection of demand and the sequence of connection and disconnection, with different load models and compositions, should be performed prior to developing and deploying optimal DSM strategy for a given system.

## ACKNOWLEDGMENT

This research is partly supported by the Department of Electrical and Electronic Engineering of The University of Manchester and partly by the EU Horizon 2020 project CROSSBOW (Grant No.:773430).

The authors gratefully acknowledge the contributions of Dr. A. Adrees and Dr. P. Papadopoulos to the test network modifications and development of loading scenarios.

This paper only reflects the authors' view and neither the Agency nor the Commission are responsible for any use that may be made of the information contained therein.

## REFERENCES

[1] M. T. Muhssin, L. M. Cipcigan, S. S. Sami and Z. A. Obaid, "Potential of demand side response aggregation for the stabilization of the grid frequency," *ELSEVIER*, Applied Energy 220, pp. 643-656, 2018.

[2] H. W. Qazi and D. Flynn, "Analysing the impact of large-scale decentralised demand side response on frequency stability," *ELSEVIER*, Electrical Power and Energy Source 80, pp. 1-9, 2016.

[3] S. E. D. Coalition, "Mapping demand response in Europe today," *Tracking Compliance with Article*, Vol. 15, 2014.

[4] CIGRE WG C4.605: "Modelling and aggregation of loads in flexible power networks," Jovica V. Milanovic, (Convenor), (TB 566), ISBN: 978-2-85873-261-6, February 2014.

[5] P. Kundur, J. Paserba, V. Ajjarapu, G. Andersson, A. Bose, C. Canizares, N. Hatziargyrious, D. Hill, A. Stankovic, C. Taylor, T. V. Cutsem and V. Vittal. "Definition and classification of power system stability IEEE/CIGRE joint task force on stability terms and definitions," *IEEE Trans. Power Systems*, vol. 19, pp. 1387-1401, May 2004

[6] "Assessment of Industrial Load for Demand Response across U.S. Regions of the Western Interconnected," *Oak Ridge National Laboratory*, 2013.

[7] The University of Edinburgh, "Matching Renewable Electricity Generation with Demand," Scottish Executive, Edinburgh, 2006.

[8] G. Rogers, *Power System Oscillations*. Norwell, MA, USA: Kluwer, 2000.

[9] S. Tao, Y. Ruoying, Z. Lingzhi and G. Shan, "Power system probabilistic production simulation containing large-scale wind power and photovoltaic power," in *Proc. IEEE PES Asia-Pacific Power Energy Eng. Conf.*, pp. 1-6, Dec. 8-11, 2013.

[10] M. Fan, V. Vittal, G. Heydt and R. Ayyanar, "Probabilistic power flow studies for transmission systems with photovoltaic generation using cumulants," *IEEE Trans. Power Systems*, vol. 27, no. 4, pp. 2251-2261, Nov. 2012.

[11] T. Guo and J. V. Milanovic, "Probabilistic framework for assessing the accuracy of data mining tool for online prediction of transient stability," IEEE Trans. Power Systems, vol. 29, no.1, pp. 318-326, Feb. 2014.

[12] M. Wang, J. Ponocko and J. V. Milanovic, "The Effect of the Type and Composition of Demand on the Influence of DSM on Power System Angular Stability," *IEEE PES GTD Grand International Conference and Exposition Asia*, March 21-23 2019.

[13] "Modelling and Aggregation of Loads in Flexible Power Networks," CIGRE WG C4.605, 2013.

[14] I. Richardson, M. Thomson, D. Infield and C. Clifford, "Domestic electricity use: A high-resolution energy demand model," *Energy and Buildings*, vol. 42, pp. 1878-1887, 2010.

[15] R. D. Zimmerman, C. E. Murillo-Sanchez and R. J. Thomas, "MATPOWER: Steady-state operations, planning and analysis tools for power system research and education," *IEEE Trans. Power Systems*, vol. 26, no. 1, pp. 12-19, Feb. 2011.

[16] R. Preece and J. V. Milanovic, "Efficient estimation of the probability of small-disturbance instability of large uncertain power systems", *IEEE Trans. Power Syst.*, vol. 31, no. 2, pp. 1063-1072, Mar. 2015.